



Article

Innovative Design Techniques for Sinusoidal-Web Beams: A Reliability-Based Optimization Approach

Imre Cserpes, Muayad Habashneh, János Szép  and Majid Movahedi Rad * 

Department of Structural and Geotechnical Engineering, Széchenyi István University, 9026 Győr, Hungary; cserpesi@sze.hu (I.C.); habashneh.muayad@sze.hu (M.H.); szepj@sze.hu (J.S.)

* Correspondence: majidmr@sze.hu

Abstract: Existing studies often rely on deterministic numerical analyses for structural models. However, test results consistently highlight uncertainties, particularly in variables such as magnitude of the applied load, geometrical dimensions, material randomness, and limited experiential data. As a response, researchers have increasingly turned their attention to probabilistic design models, recognizing their crucial role in accurately predicting structural performance. This study aims to integrate reliability-based analysis into the numerical modeling of sinusoidal-web steel beams. Two sinusoidal-web beams are considered. The web and the flange thicknesses, in addition to the magnitude of the applied load, are treated as random variables with mean values and standard deviations. Notably, the study demonstrates the efficiency of the reliability index as a governing limit in the analysis process. A detailed comparison between deterministic and probabilistic designs of sinusoidal-web beams is conducted, focusing on the impact of introducing the nature of randomness. Therefore, this study's results deepen our understanding of how uncertainties significantly influence deformations and stresses.

Keywords: sinusoidal-web beams; structural optimization; reliability design; probabilistic analysis; parametric design



Citation: Cserpes, I.; Habashneh, M.; Szép, J.; Movahedi Rad, M. Innovative Design Techniques for Sinusoidal-Web Beams: A Reliability-Based Optimization Approach. *Buildings* **2024**, *14*, 1051. <https://doi.org/10.3390/buildings14041051>

Academic Editor: André Rafael Dias Martins

Received: 29 December 2023

Revised: 27 March 2024

Accepted: 4 April 2024

Published: 9 April 2024



Copyright: © 2024 by the authors. Licensee MDPI, Basel, Switzerland. This article is an open access article distributed under the terms and conditions of the Creative Commons Attribution (CC BY) license (<https://creativecommons.org/licenses/by/4.0/>).

1. Introduction

Steel beams are integral components within the area of structural engineering, assuming a crucial role by furnishing indispensable support and stability across a diverse array of constructions. Serving as foundational elements, these beams bear the weight of structures with unwavering resilience, ensuring the structural integrity required for the complex interplay of forces and loads in various engineering applications [1–4].

There has been an increasing emphasis, in recent years, on the innovative design of steel beams with corrugated webs, marking a departure from traditional beam configurations [5,6]. By analyzing the results of finite element analysis and reliability analysis in order to compute the capacity factor, Papangelis et al. [6] developed a design framework for beams featuring corrugated webs. Driver et al. [7] proposed a lower limit equation that accounts for web deformation in both the elastic and inelastic domains when designing steel I-girders featuring corrugated webs. Furthermore, Hassanein et al. [8] examined steel girders that were constructed using high-strength steels and had corrugated web plates. The purpose was to develop constructions that were both slender and efficient in terms of weight. To evaluate the fatigue behavior of corrugated-web girders, Ibrahim et al. [9] conducted an experiment, establishing a relationship between stress and cycle and comparing the results to AASHTO specifications.

Weight reduction and resistance to buckling have contributed to the increased use of corrugated web beams, particularly those featuring sinusoidal corrugation, in the primary frameworks of single-story steel buildings [10]. This unique geometry offers distinct advantages in terms of load distribution and structural efficiency. The impact that critical geometric parameters have on steel beams' performance, particularly those with sinusoidal

webs, has been comprehensively explored. These studies investigated the intricate relationships between beam geometry, material properties, and structural behavior, laying the groundwork for a deeper understanding of the sinusoidal-web configuration [11–13]. The failure modes, shear strength, rigidity, and strain distributions of girders manufactured from steel featuring corrugated webs were the subject of experimental and computational investigations in a study by Wang et al. [14]. Using validated models, Lee et al. [15] performed a nonlinear finite element analysis to examine sinusoidal webs and trapezoidal web beams. In their study, Zhang et al. [16] examined the flexural behavior of wide-flange members whose webs featured sinusoidal corrugations. Pathirana and Qiao [17] examined the local buckling behavior of sinusoidal panels at different aspect ratios, corrugated amplitudes, and thicknesses. Furthermore, Nikoomanesh and Goudarzi [18] conducted experimental and numerical investigations to determine the capacity for ultimate shear in sinusoidal web beams. By concentrating on shear buckling stress and failure modes, Kim and Park [19] examined the sensitivity analysis of sinusoidal steel webs and discovered a specific correlation between design variables. Sebastiao and Papangelis [20] employed finite element analysis to calculate the elastic shear deformation of beams featuring sinusoidal corrugated webs. By considering the aim of increasing the shear capacity of narrow plates in a fabrication-intensive manner, Wang et al. [21] suggested a method for generating low-frequency sinusoidal patterns on the plate. Corrugated-web steel beams and traditional steel beams exhibited comparable failure forms, according to the study of Górecki and Śledziewski [22] on steel plate girders; however, the corrugated steel webs in bridge girders were thinner than conventional solutions.

Reliability-based design approaches have emerged as indispensable tools in ensuring the structural integrity of engineering systems [23–26]. In the context of steel beams, particularly those featuring sinusoidal webs, a robust examination of reliability becomes imperative. Pimenta et al. [27] provided reliability-based design guidelines for sinusoidal-web beams, including theoretical models, experimental studies, and finite element models. Leblouba and Tabsh [28] examined the absence of a design strategy that focuses on reliability for sinusoidal-web beams. This was carried out by analyzing reliability indices and adjusting resistance components. By comparing the results of deterministic and stochastic nonlinear analyses, Bärnkopf et al. [29] discerned the precise buckling resistance and assessed the structural behavior of steel corrugated-web girders prior to examining their failure mode. Pimenta et al. [30] provided design guidelines for composite sinusoidal-web beams and their connections, based on a reliability-based design.

Expanding on the insights acquired from parametric studies and reliability-based designs, the optimization of structures [31,32], with a specific focus on the integration of sinusoidal-web steel beams, has become a central theme in contemporary structural engineering research [33]. With an emphasis on the corrugated web I-girder, Sokołowski and Kamiński [34] introduced a framework for the topological optimization of corroding structures, based on a reliability-based design. By concentrating on the optimal weight design and parameter effects, Shon et al. [35] developed an optimization algorithm for sinusoidal-web steel beams. Shon et al. [36] investigated the optimal design of corrugated web steel beams, aiming to increase their strength and adaptability to a variety of structures. Furthermore, Lee et al. [37] investigated the optimal weight design for sinusoidal web beams. By incorporating variables such as thicknesses of web and flange and height into a stochastic optimization algorithm, Erdal et al. [38] proposed an algorithm to find the most effective configuration for the considered beams.

By conducting an exhaustive investigation, this study intends to determine the impact of incorporating a reliability-based optimization design into the numerical analysis of sinusoidal-web steel beams. Unveiling the optimal design parameters for sinusoidal-web steel beams is proposed through a series of analyses and comparisons. The intricate nature of sinusoidal-web geometry poses a distinct challenge and promises novel insights into optimal design parameters. Initially, a comparison between the results obtained from numerical analyses and experimental tests to validate our finite element models is

presented. Subsequently, the optimal design parameters for sinusoidal-web steel beams, through a series of analyses and comparisons, are discussed. Furthermore, the research investigates the results of four-point bending experiments conducted on the two beam models under investigation. In order to accomplish the desired objective, probabilistic analysis is performed using a nonlinear-written code, under the assumption that the introduced reliability index serves as a constraint, when random variations in geometrical dimensions and the magnitude of applied loads are considered. In addition, reliability indices are calculated utilizing the Monte Carlo method in accordance with the statistical characteristics of sinusoidal-web properties.

2. Theoretical Background

2.1. Finite Element Analysis

This paper examines the problems associated with sinusoidal-web steel beams through numerical investigation, incorporating imperfect nonlinear analysis. This particular analysis takes into consideration elastoplastic relations and large displacements, in accordance with the shell bending theory.

ABAQUS 2018 [39] software is employed to analyze the linear buckling analysis, for which the considered geometrical imperfections are regarded as a linear combination of the eigenvectors. Furthermore, the method that has been proposed may be deemed a rational approach to estimate imperfections in geometry.

Although numerous papers have been published in the domain of finding the minimum collapsing load, the aim of the methodology employed in this particular paper does not purport to determine the minimum collapse load. Conversely, this research examines the optimization reaction of a delicate defective structure when confronted with probabilistic problems.

2.2. Reliability-Based Optimization Framework

Referring to the fundamental concept of reliability analysis, this study employs a design founded on reliability. Assuming X_S and X_R are two independent random variables with probabilistic density functions $f_R(X_S)$ and $f_R(X_R)$, respectively, the failure criterion can be approximated as $X_R \leq X_S$, where X_R represents the non-negative limit for X_S . Equation (1) is, therefore, employed to approximate the failure probability (P_f) [40].

$$P_f = P[X_R \leq X_S] = \iint_{X_R \leq X_S} f_R(X_R) f_S(X_S) dX_R dX_S \quad (1)$$

The previous equation, which is defined with respect to the limit state function, can be subject to an alternative definition:

$$g(X_R, X_S) = X_R - X_S \quad (2)$$

The failure domain, D_f , is characterized by $g \leq 0$. In order to derive P_f , the subsequent expression is employed:

$$P_f = F_g(0) \quad (3)$$

Furthermore, it is possible to express P_f as:

$$P_f = \int_{g(X_R, X_S) \leq 0} f(X) dX = \int_{D_f} f(X) dX \quad (4)$$

This research employs a mathematical technique known as the Monte Carlo method to estimate the P_f distribution. By utilising the probability joint density function, $f_X(x)$, the fundamental concept underlying this approach is to generate the random vector X . The Monte Carlo method enables the estimation of P_f by calculating the ratio between the number of points generated and the total number of points within the failure domain. In-

incorporating the indicator function of D_f into the formulation that expresses this hypothesis yields the following:

$$\chi_{D_f}(x) = \begin{cases} 1 & \text{if } x \in D_f \\ 0 & \text{if } x \notin D_f \end{cases} \quad (5)$$

Therefore, it is possible to reconstruct the P_f formula as follows:

$$P_f = \int_{-\infty}^{+\infty} \dots \int_{-\infty}^{+\infty} \chi_{D_f}(x) f_X(x) dx \quad (6)$$

Consequently, the random variable $\chi_{D_f}(X)$ exhibits a two-point distribution:

$$\mathbb{P}[\chi_{D_f}(X) = 1] = P_f \quad (7)$$

$$\mathbb{P}[\chi_{D_f}(X) = 0] = 1 - P_f \quad (8)$$

where P_f is equal to $\mathbb{P}[X \in D_f]$. $\chi_{D_f}(X)$ is correlated with the mean value and variance, which are ascertained as follows:

$$\mathbb{E}[\chi_{D_f}(X)] = 1 \cdot P_f + 0 \cdot (1 - P_f) = P_f \quad (9)$$

$$\text{Var}[\chi_{D_f}(X)] = \mathbb{E}[\chi_{D_f}^2(X)] - (\mathbb{E}[\chi_{D_f}(X)])^2 = P_f - P_f^2 = P_f(1 - P_f) \quad (10)$$

In the Monte Carlo technique, an estimator of the mean value to determine P_f is expressed as follows:

$$\hat{\mathbb{E}}[\chi_{D_f}(X)] = \frac{1}{Z} \sum_{z=1}^Z \chi_{D_f}(X^{(z)}) = \hat{P}_f \quad (11)$$

in which $X^{(z)}$ denotes the probability density functions associated with independent random vectors ($z = 1, \dots, Z$). Web and flange thicknesses of sinusoidal-web steel beams and the magnitude of the applied loads are regarded as random variables with a Gaussian distribution consisting of a mean value (\mathbb{E}) and variance (Var) for the purpose of accounting for uncertainties. As a result, the mean value and variance of the estimator are computed as follows:

$$\mathbb{E}[\hat{P}_f] = \frac{1}{Z} \sum_{z=1}^Z \mathbb{E}[\chi_{D_f}(X^{(z)})] = \frac{1}{Z} Z P_f = P_f \quad (12)$$

$$\text{Var}[\hat{P}_f] = \frac{1}{Z^2} \sum_{z=1}^Z \text{Var}[\chi_{D_f}(X^{(z)})] = \frac{1}{Z^2} Z P_f (1 - P_f) = \frac{1}{Z} P_f (1 - P_f) \quad (13)$$

Initial-order reliability methods, represented by the Greek letter beta (β) [40], are employed in practical structures to account for the challenges associated with precisely calculating the probability of failure. These methods utilize a metric called the reliability index. There are several benefits associated with the utilization of a reliability index. For instance, structural engineering standards provide a diverse selection of target values and a reliability-based design has been widely implemented in the field. Furthermore, the target reliability index is implemented in more routine structural engineering practices (e.g., EN1990 [41]).

In order to illustrate the reliability bounds, one may contemplate the reliability index, β , as follows:

$$\beta_{\text{target}} - \beta_{\text{calc}} \leq 0 \quad (14)$$

The subsequent equations are implemented to ascertain β_{target} and β_{calc} :

$$\beta_{\text{target}} = -\Phi^{-1}(P_{f,\text{target}}) \quad (15)$$

$$\beta_{\text{calc}} = -\Phi^{-1}(P_{f,\text{calc}}) \quad (16)$$

In the present work, the principal aim is the minimization of beam weight. Consequently, the proposed reliability-based optimization algorithm is articulated as follows:

$$\text{Minimize : } W(x) = \rho L(2A_f + A_w) = \rho L(2b_f t_f + b_w t_w) \quad (17a)$$

$$\sigma_i^C \leq \sigma_i \leq \sigma_i^T \quad (17b)$$

$$u_{\text{calc}} \leq u_{\text{target}} \quad (17c)$$

$$\beta_{\text{target}} - \beta_{\text{calc}} \leq 0 \quad (17d)$$

Here, $W(x)$ represents the total weight of the beams; ρ is the density of the material and, in our case, it is equal to 78.5 kN/m^3 ; L signifies the length of the beams; and A_f and A_w refer to the cross-sectional areas of the flange and web, respectively. Furthermore, b_f and t_f represent the width and thickness of the flange, while b_w and t_w stand for the width and thickness of the web. These geometric parameters are considered as random variables following a normal distribution, each of them has a mean value and standard deviation. Further explanation of the random variables under consideration will be provided later in the results and discussion section of this paper. It is noteworthy that, in order to maintain the structural integrity within the fully elastic zone, upper stress, σ_i^T , and lower stress, σ_i^C , bounds are employed. This precaution is implemented to prevent any plastic deformation in the resulting beams. Moreover, the displacement value is serving as a critical constraint. Notably, the termination criterion related to the displacement is defined in Equation (17c), where u_{target} represents the specified displacement limit, which should not exceed the calculated displacement value, u_{calc} , for each iteration.

3. Experimental Work

In both experiments detailed in this section, steel beams with sinusoidal-web configurations were employed. The first experiment evaluates the SIN-240 beam, and the second experiment investigates the SIN-100 beam. The beams undergo evaluation through the implementation of four-point bending experiments. The material properties utilized in this study differ for the flange part and the sinusoidal-web plate. For the flange part, the yield strength (f_y) and ultimate strength (f_u) are recorded as 288 MPa and 636.6 MPa, respectively. In contrast, the sinusoidal-web plate exhibits slightly different material properties, with a yield strength (f_y) of 282 MPa and an ultimate strength (f_u) of 639 MPa. It is pertinent to note that tensile testing of stainless steel sheets was conducted at ambient temperature in order to obtain the mechanical properties of the selected material, with the resultant force-displacement curves depicted in Figure 1.

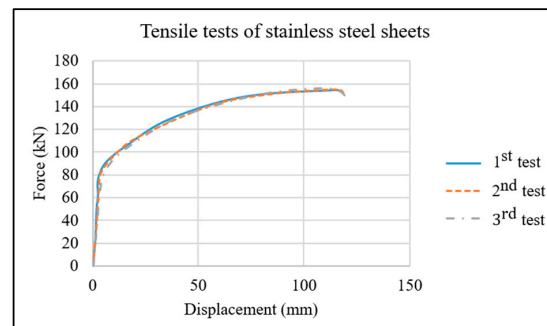


Figure 1. Force-displacement curves of the tensile tests of the considered stainless steel sheets.

For the experimental tests, we selected six sinusoidal-web steel beams, with three identified as SIN-240 beams. Each SIN-240 beam features a 10 mm flange thickness (t_f), a flange width (b_w) of 120 mm, a 2 mm thickness of the sinusoidal-web plate (t_w), and a

height (h) of 240 mm. Furthermore, we standardized the length of each beam (L) to be 4000 mm. The other three sinusoidal-web steel beams were identified as SIN-100 beams, with the following characteristics: 6 mm flange thickness (t_f), a flange width (b_w) of 55 mm, a 1.5 mm thickness of the sinusoidal-web plate (t_w), a height (h) of 100 mm, and a total length (L) equal to 4000 mm. Furthermore, the experimental test layout and the schematic of SIN-240 and SIN-100 beams are represented in Figures 2 and 3, respectively. The considered geometry of the sinusoidal wave is the same for both beams, as is illustrated in Figure 4. In light of the various experimental analyses, the outcomes obtained in conjunction with the designated material affirm the appropriateness of the 40 mm width within our study. The selected dimensionality not only effectively resists local effects but also serves as a mitigating factor against torsional buckling. These findings are substantiated by a comprehensive examination of the structural behavior, wherein the prescribed width demonstrates a notable resilience and efficacy in addressing localized stressors. Through meticulous observation and empirical validation, our research establishes the paramount significance of this particular dimension, contributing to the overall robustness and stability of the structural elements under scrutiny. Furthermore, the experimental data underscore the material's capacity to withstand torsional forces, thus affirming the judicious choice of the specified width in fostering structural integrity and performance resilience. Furthermore, in order to provide a comprehensive understanding of the physical characteristics of the tested specimens, the detailed dimensions are presented in Table 1. Notably, the lengths, widths, heights, and thicknesses of the specimens, including SIN-240 and SIN-100, are outlined, facilitating a more nuanced examination of their structural properties.

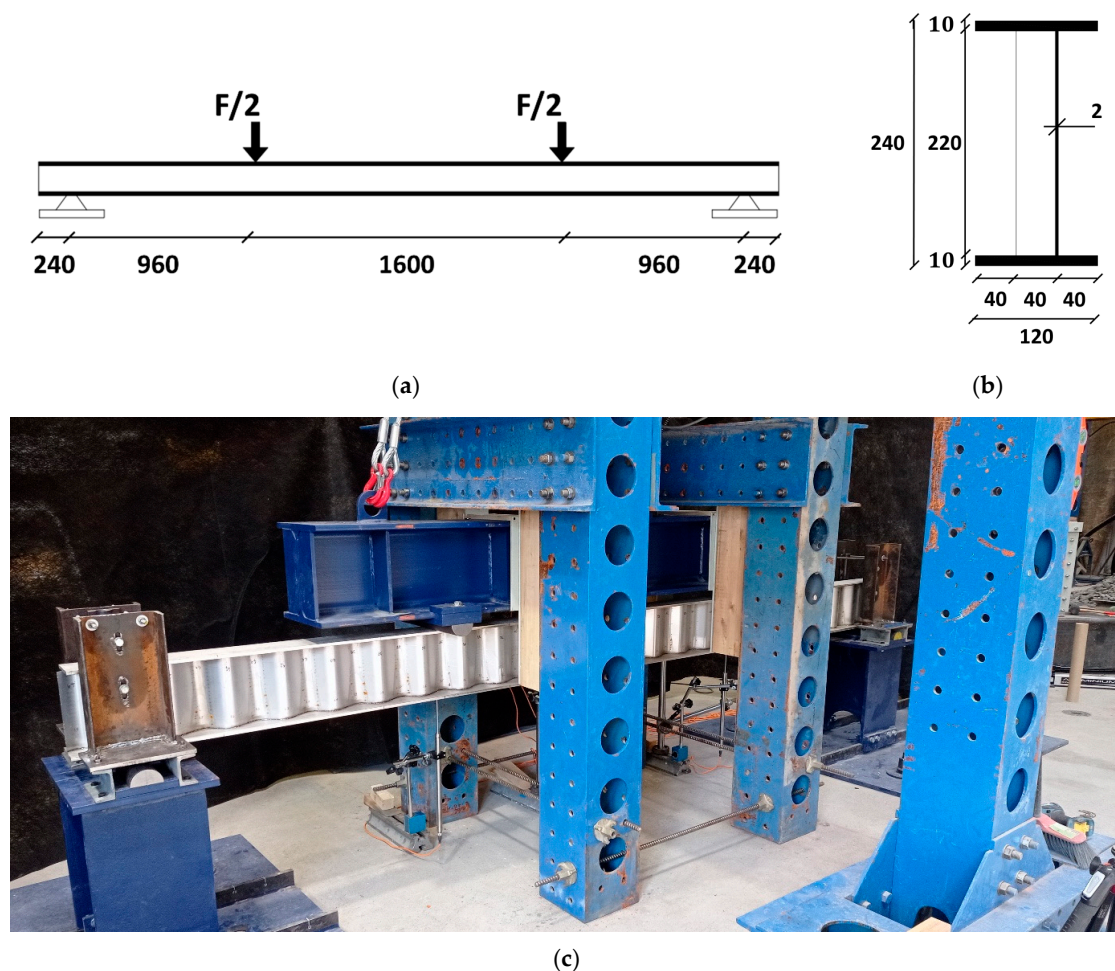


Figure 2. SIN-240 beams: (a) Geometry and the boundary conditions. (b) Cross-section. (c) Experimental test layout.

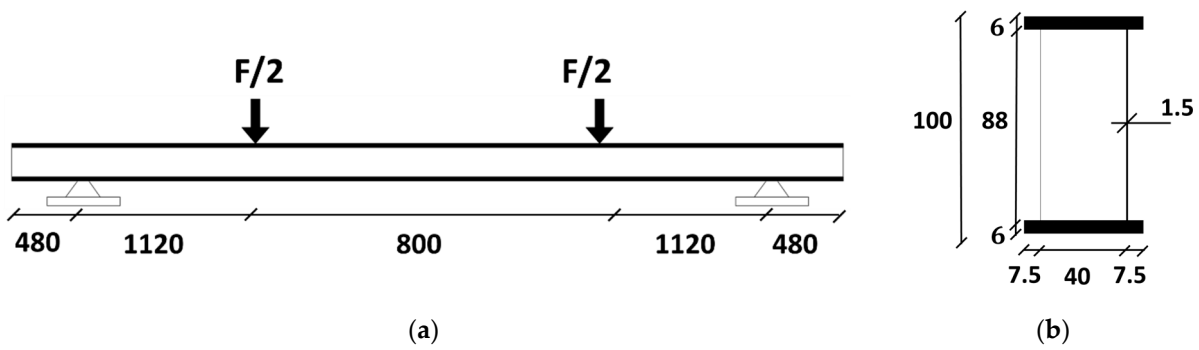


Figure 3. SIN-100 beams: (a) Geometry and the boundary conditions. (b) Cross-section. (c) Experimental test layout.

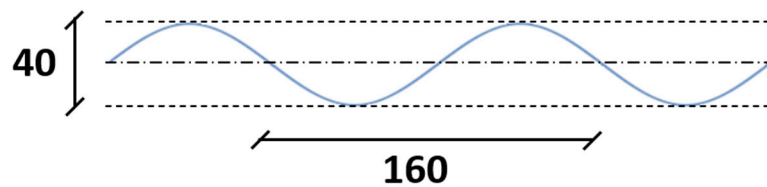


Figure 4. Considered geometry of the sinusoidal wave.

Table 1. Dimensions of tested specimens.

Specimen Name	Length (mm)	Width (mm)	Height (mm)	Flange Thickness (mm)	Web Thickness (mm)
SIN-240	4000	120	240	10	2
SIN-100	4000	55	100	6	1.5

In the experimental investigation detailed in this chapter, an essential aspect of our analysis pertains to the failure modes observed in the steel beams. The structural response under loading conditions led to localized failures, particularly near the loading points. This phenomenon is attributed to the combined effect of bending and shear forces. The failure mechanisms were predominantly localized, emphasizing the significance of understanding the intricate interplay between bending and shear in the context of steel structural elements.

4. Numerical Modeling

This section proposes the utilization of finite element analysis (FEA) in conjunction with the commercial FEA software ABAQUS [39]. The objective is to model the imperfect nonlinear behavior exhibited by sinusoidal-web steel beams. By employing FEA and ABAQUS, we aim to capture and analyze the intricate structural response of these beams under various loading conditions. This approach allows for a comprehensive examination of the nuanced deformations and stresses, providing valuable insights into the performance of sinusoidal-web steel beams in real-world applications. Moreover, both beams are simulated using four-sided finite membrane strain (S4) elements, as illustrated in Figure 5. This modeling approach permits the alteration of shell thickness in tandem with the deformation of the elements.

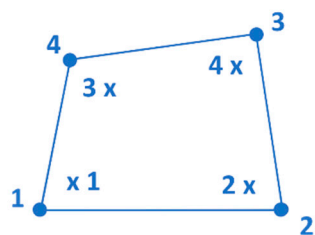


Figure 5. Considered 4-node full integration element for FEA.

In the context of our numerical analysis, it is imperative to reiterate that the introduced imperfection aligns with the major axis, and its positive direction is considered. Through meticulous examination of the sinusoidal profiles inherent in our structural elements, we have discerned that these models exhibit a robust insensitivity to torsional imperfections specific to these cross-sections. This observation underscores the unique behavior of sinusoidal-web steel beams, providing valuable insights into their structural response. Furthermore, all material properties employed in our numerical models are derived directly from experimental tests. Rigorous testing procedures have been conducted to comprehensively characterize the material's mechanical behavior under varying loading conditions. This ensures the accuracy and reliability of the material properties utilized in our simulations, contributing to the overall fidelity of our numerical predictions.

4.1. SIN-240

The ABAQUS model of the SIN-240 beam is illustrated in Figure 6, where the applied load acts at two positions. The boundary conditions are considered as a pinned-fixed connection, supplemented by lateral supports, to accurately emulate the experimental test conditions. The proposed numerical model is discretized into 6450 elements to produce an improved mesh for this part, reliable results are guaranteed. In the analysis of linear buckling, a perturbation with an imperfection value equivalent to $L/1000$ has been incorporated. This imperfection serves as a crucial factor in assessing the stability of the structure under various loading conditions. The consequential global buckling mode, which signifies the structural response to this imperfection, is visually represented in Figure 7.

The experimental outcomes were utilized to validate the numerical results of the model. The analysis reveals a substantial degree of concurrence, as depicted in Figure 8. In Figure 9, it is evident that the observed failure mode aligns closely with web crippling. Furthermore, the failure occurred in the region surrounding the points of applied load and the ratio (σ/σ_y) provides a measure of the material's stress level relative to its yield stress.

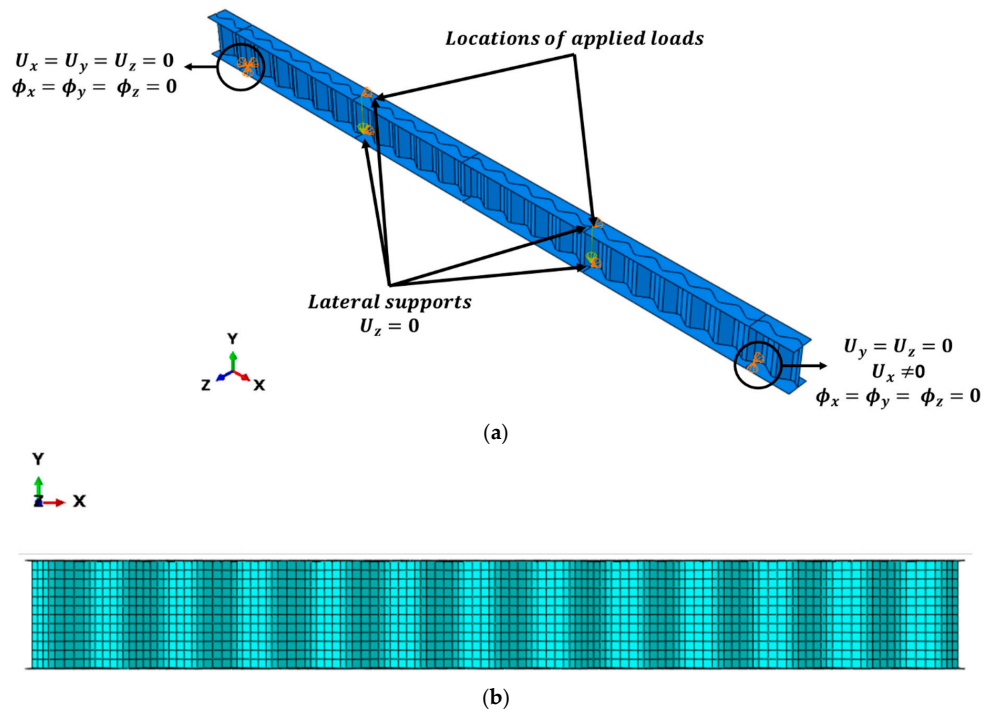


Figure 6. SIN-240 numerical model. (a) Model assembly. (b) Mesh of the model.

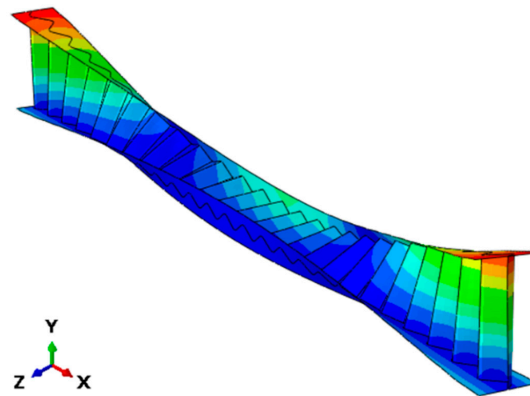


Figure 7. Considered global buckling mode.

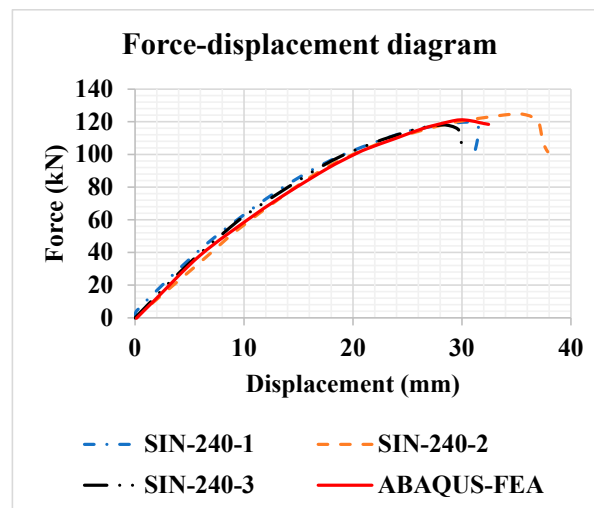


Figure 8. Force-displacement diagrams of SIN-240.

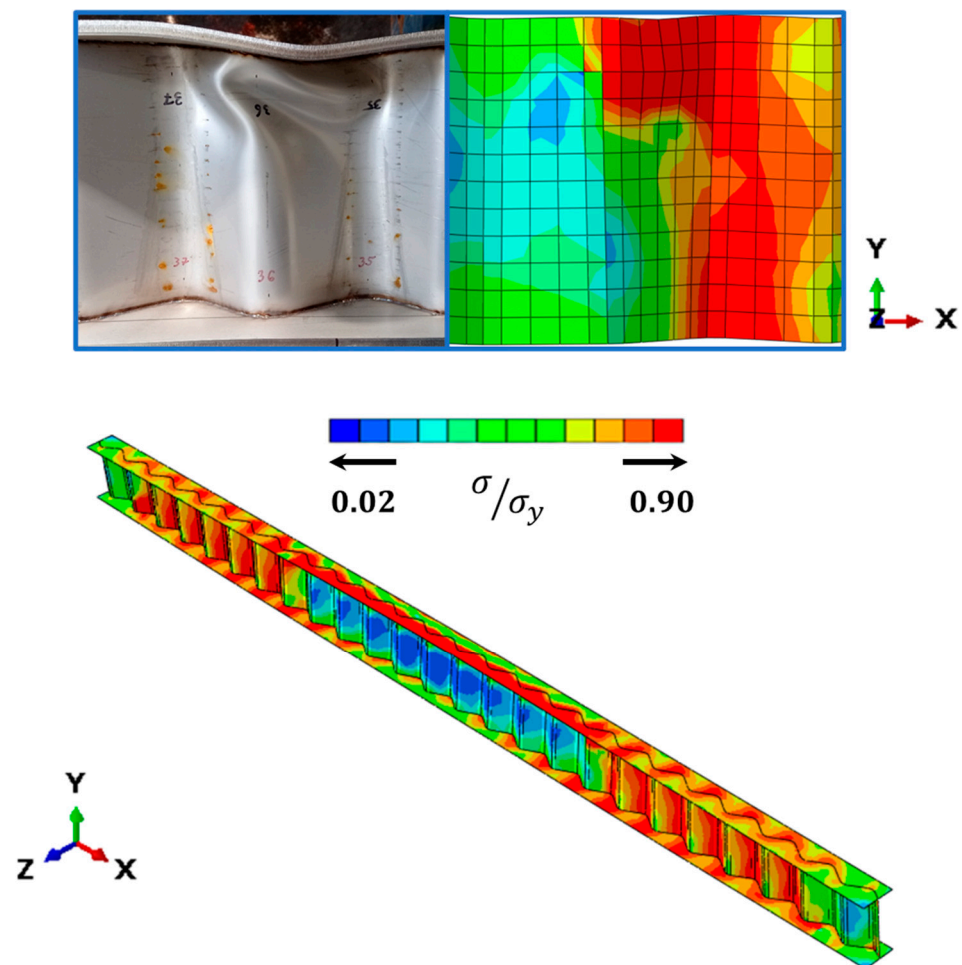


Figure 9. The observed failure mode in the case of SIN-240.

4.2. SIN-100

The ABAQUS model for the SIN-100 beam is depicted in Figure 10, showcasing the application of the load at two distinct positions. The boundary conditions are defined with a pinned-fixed connection and additional lateral supports, mirroring the experimental test conditions accurately. To enhance the mesh quality and ensure reliable results, the numerical model is discretized into 5500 elements. In the examination of linear buckling, the analysis incorporates a perturbation with an imperfection value of $L/1000$. This deliberate imperfection plays a vital role in evaluating structural stability under diverse loading conditions. The resulting global buckling mode, illustrating the structural response to this imperfection, is visually presented in Figure 11.

The numerical model for the SIN-100 beam underwent validation using experimental data. The comparison, as illustrated in Figure 12, demonstrates a significant concurrence between the experimental and numerical outcomes. Specifically, the characteristic failure in the case of the SIN-100 beam occurs within the beam as a consequence of the compressed flange buckling in the region between the applied forces; the ratio (σ/σ_y) offers a gauge of the material's stress magnitude in relation to its yield stress, as is clearly evident in Figure 13.

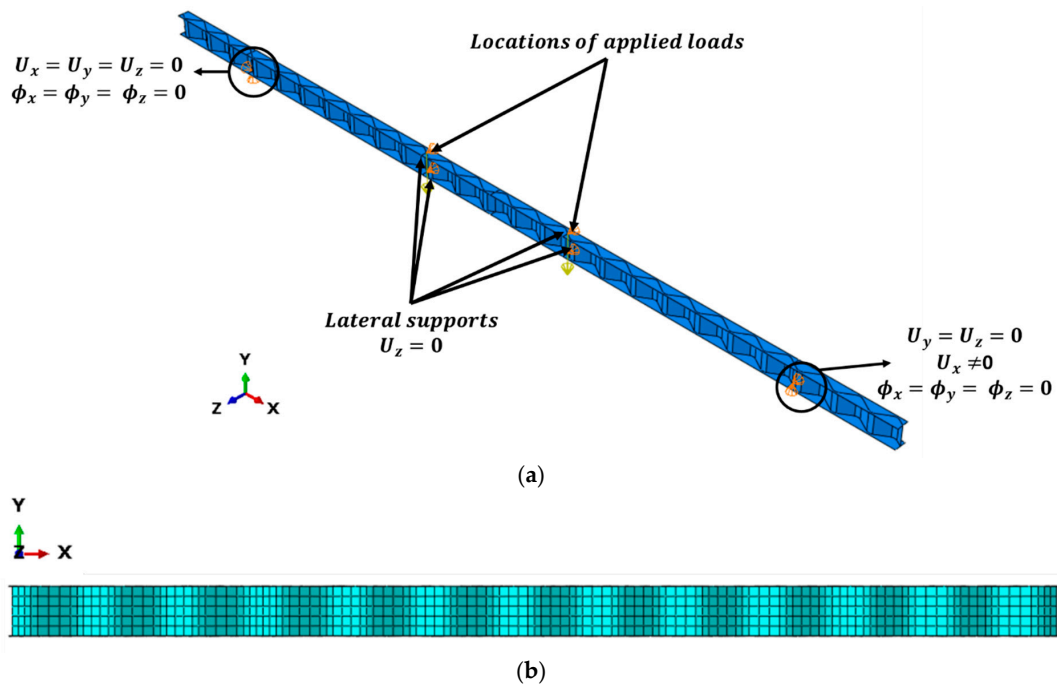


Figure 10. SIN-100 numerical model. (a) Model assembly. (b) Mesh of the model.

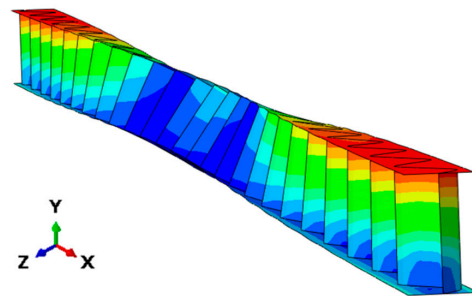


Figure 11. Considered global buckling mode.

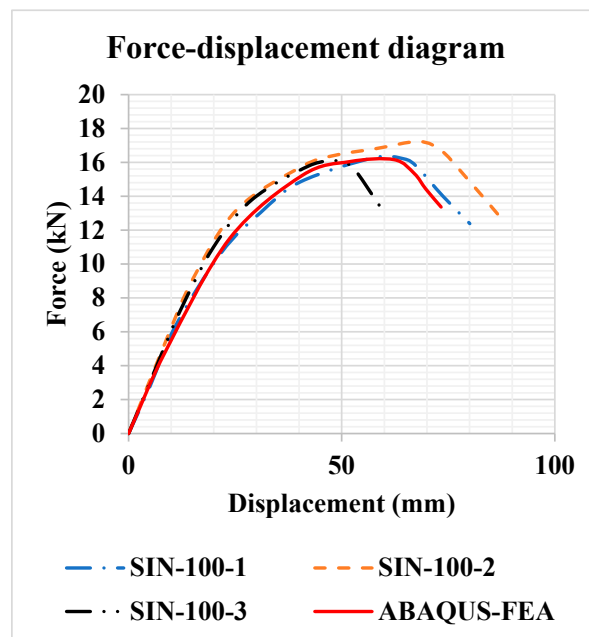


Figure 12. Force-displacement diagrams of SIN-100.

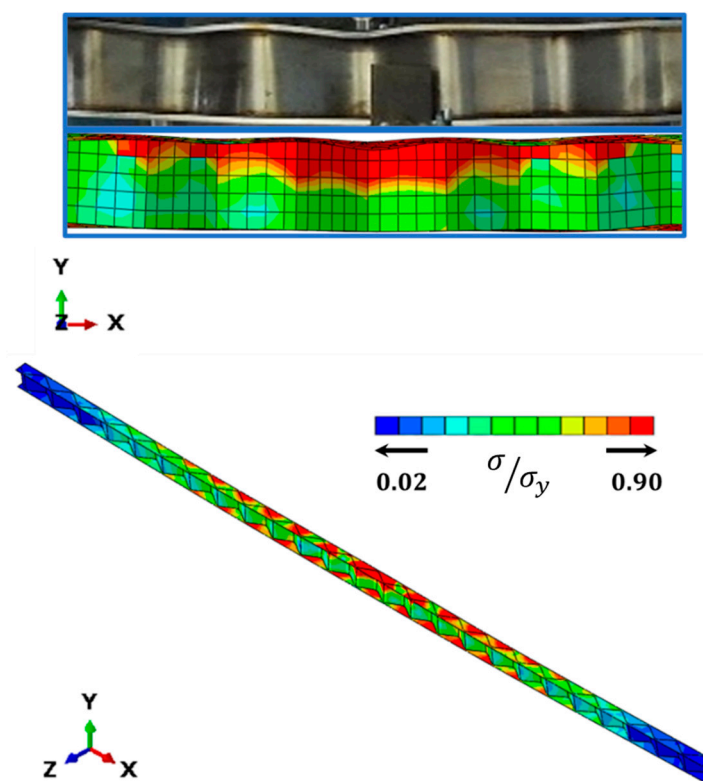


Figure 13. The observed failure mode in the case of SIN-100.

5. Results and Discussion

This section presents an in-depth analysis of the data gathered from both the SIN-240 and SIN-100 beams, offering a comprehensive comparison of these findings. We employ the FEA program ABAQUS to assess the numerical models using data obtained from experimental experiments, as previously mentioned. Subsequently, we develop a code to conduct probabilistic analysis, assuming that the newly introduced reliability index acts as a constraint. The analysis takes into account random factors, such as the thickness of the flanges, the thickness of the sinusoidal-web plate, and the magnitude of the applied loads, each characterized by their mean values and standard deviations. For the calculation of reliability indices, we employ the Monte Carlo technique, assuming a total sample point number ($Z = 3 \times 10^7$). Furthermore, the assumed random variables are shown in Table 2.

Table 2. Considered random variables of the considered beams.

Beam	Parameter	Mean Value	Standard Deviation
SIN-240	t_f (mm)	10	40%
	t_w (mm)	2	35%
	F (kN)	90	5%
SIN-100	t_f (mm)	6	40%
	t_w (mm)	1.5	35%
	F (kN)	12	5%

It is important to note that upon the completion of numerous simulations for both beams, it has been observed that the inclusion of imperfections as a random variable does not exert a significant impact on the obtained results, as the mean values of the applied load are below the ultimate load-bearing capacities. As a consequence, a deliberate decision has been made to exclude imperfections from the analysis, with a focus on variables that bear a more substantial influence on the structural behavior. Furthermore, the overarching goal of achieving an optimal and sustainable design is emphasized in the research. The iterative

process of running simulations has served to fortify the understanding that structural efficiency and material savings can be achieved without compromising reliability. This aligns with the ethos of responsible material utilization, a cornerstone of contemporary steel structural engineering practices dedicated to sustainable design principles.

5.1. SIN-240 Results Overview

Within the paradigm of reliability-based optimization specific to the SIN-240 sinusoidal-web steel beam, the interplay between finite element analysis (FEA) and advanced optimization techniques becomes vital. The application of a reliability-based optimization algorithm, complemented by Monte Carlo simulation, is pivotal for steering the structural design toward a robust configuration capable of withstanding unforeseen variations in load and environmental conditions.

The analysis of the SIN-240 beam yields three distinct outcomes based on varying reliability index (β_{target}) values, as illustrated in Table 3. It is evident that the introduction of β_{target} serves as a constraint, dictating how alterations in thickness affect both the load (F) and the corresponding displacement (U). Notably, there is a reduction of 10.14% in displacement values, from 20.00 mm when $\beta_{\text{target}} = 3.00$ to 18.16 mm when $\beta_{\text{target}} = 4.00$. Moreover, opting for lower β_{target} values correlates with increased loads and, subsequently, larger displacements. This underscores how the study incorporates uncertainties stemming from the randomness of web and flange thicknesses, manifesting in varied properties across iterations.

Table 3. Results of SIN-240.

β_{target}	t_f (mm)	t_w (mm)	F (kN)	U (mm)
4.00	10.00	2.5	87.3	18.16
3.55	10.00	1.50	88.89	19.82
3.00	6.00	2.00	92.90	20.00

The mean applied load of 90 kN, as indicated in Table 2, serves as a reference point within the elastic range. The subsequent observation of a slightly elevated load of 92 kN during the analysis highlights the inherent variability in real-world scenarios. The resultant displacement measure of 19.5 mm, leading to program termination, underscores the algorithm's sensitivity to deviations from expected structural behavior. This sensitivity is a cornerstone in pre-emptively identifying potential failure modes, safeguarding the structural integrity of the SIN-240 beam.

The convergence toward optimized values, driven by a targeted reliability index ($\beta_{\text{target}} = 3.00$) stands as a testament to the efficacy of reliability-based optimization in tailoring the SIN-240 beam's design to meet stringent reliability constraints. The derived values of web thickness (t_w) and flange thickness (t_f) were 2 mm and 6 mm, respectively. It is worth mentioning that those obtained values not only ensure stability under specified conditions but also hint at an efficient utilization of materials—a crucial consideration in sustainable steel structure design. Figure 14, depicting the stress distribution of the SIN-240 optimized configuration, serves as a visual testament to the efficacy of reliability-based optimization in mitigating potential weak points within the structure. A detailed analysis of the stress distribution reveals notable improvements, particularly in the reduction in zones exhibiting yielded stress. In other words, in ensuring structural integrity and averting plastic accumulation, we rigorously enforce full elasticity across all zones in the resulting model. This is achieved through stringent constraints on the upper and lower stress bounds, playing a pivotal role in guiding the optimization process.

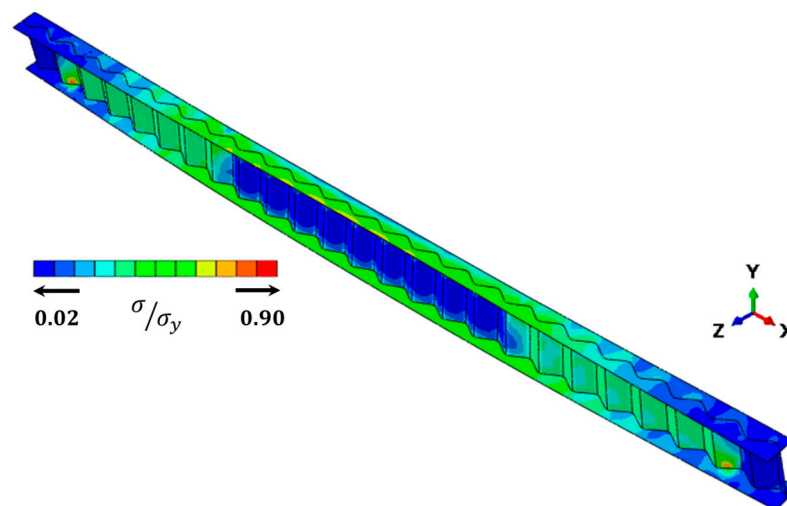


Figure 14. The stress distribution within the optimized configuration of the SIN-240 beam.

5.2. SIN-100 Results Overview

Turning our attention to the results of the second beam, specifically the SIN-100 sinusoidal-web steel beam, this section explores the intricate relationship between finite element analysis (FEA) and advanced optimization techniques within the framework of reliability-based optimization. The employment of a reliability-based optimization algorithm, coupled with Monte Carlo simulation, becomes paramount in steering the structural design towards a robust configuration capable of withstanding unforeseen variations in load and environmental conditions.

The mean applied load of 12 kN, as outlined in Table 2, serves as a benchmark within the elastic range. The subsequent identification of a slightly increased load of 12.45 kN during the analysis emphasizes the inherent variability in real-world scenarios. The resulting displacement of 26 mm, leading to the termination of the program, highlights the algorithm's sensitivity to deviations from expected structural behavior. This sensitivity is fundamental in proactively identifying potential failure modes and ensuring the structural integrity of the SIN-100 beam.

The outcomes derived for different β_{target} values are presented in Table 4. By taking into account the reliability index, adjustments in thicknesses trigger corresponding variations in both the load (F) and displacement (U) values. For instance, the displacement values exhibit a reduction of 29.55% from 26.00 mm when $\beta_{\text{target}} = 3.00$ to 20.07 mm when $\beta_{\text{target}} = 4.07$. This underscores the significance of the reliability index as a governing constraint, steering the outcomes accordingly. Echoing previous observations, the inclusion of random variables pertaining to web and flange thicknesses clarifies how the introduction of a reliability-based design influences the results, in concurrence with the acquired β_{target} values.

Table 4. Results of SIN-100.

β_{target}	t_f (mm)	t_w (mm)	F (kN)	U (mm)
4.00	8.00	2.00	9.12	20.07
3.55	6.00	2.50	9.57	24.26
3.00	6.00	1.40	12.45	26.00

In a manner analogous to the optimization process discussed earlier for the SIN-240 beam, the convergence toward optimized values remains a central theme in our current analysis. Here, driven by a targeted reliability index ($\beta_{\text{target}} = 3.00$), this process stands as a testament to the efficacy of reliability-based optimization in tailoring the design to meet stringent reliability constraints. The derived values of web thickness (t_w) and flange thickness (t_f) in this context were 1.4 mm and 6 mm, respectively. Similar to the previous

case, these values not only ensure stability under specified conditions, but also hint at an efficient utilization of materials—an essential consideration in sustainable steel structure design. This observation is further exemplified through Figure 15, depicting the stress distribution of the optimized configuration. Just as observed in the SIN-100 example, a detailed analysis of the stress distribution in this case reveals notable improvements, particularly in the reduction in zones exhibiting yielded stress. Similarly, to uphold structural integrity and prevent plastic accumulation, a strict adherence to maintaining full elasticity across all zones within the resulting model is employed. This adherence is implemented through precise constraints on the upper and lower stress bounds, serving as a crucial guide in steering the optimization process.

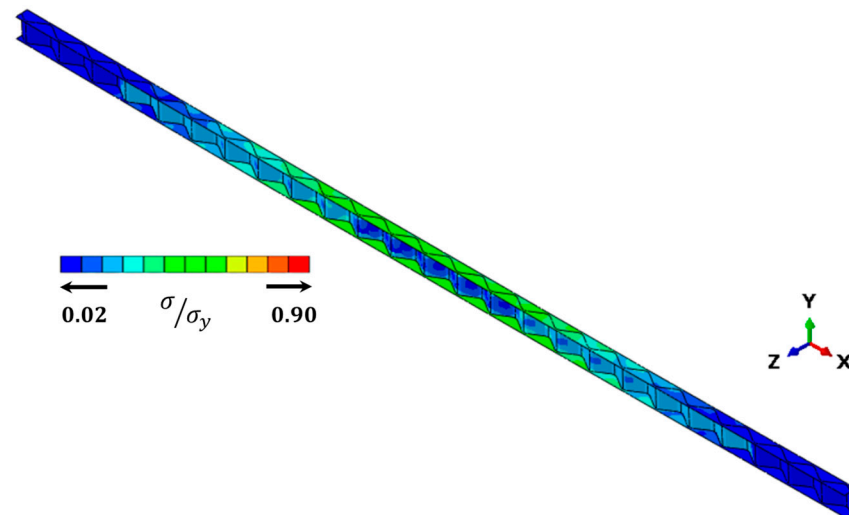


Figure 15. The stress distribution within the optimized configuration of the SIN-100 beam.

6. Conclusions

This paper introduces a method for optimizing the design of nonlinear imperfect sinusoidal-web beams based on a reliability-based design. Moreover, a written code is employed that incorporates the use of a reliability index as a controlling factor for the analysis boundary. This code takes into account the random nature of variables such as the thickness of the flanges, the thickness of the sinusoidal-web plate, and the magnitude of the applied loads, which, under the assumption, adhere to a normal distribution characterized by a mean value and standard deviation. Moreover, the application of finite element analysis (FEA) through ABAQUS software allows for a meticulous exploration of the structural response of these beams under various loading conditions. Therefore, it is evident that the reliability-based optimization, integrated with Monte Carlo simulation, plays a pivotal role in steering the structural design toward robust configurations capable of withstanding uncertainties in load and manufacturing conditions.

Drawing from the aforementioned discussion, the following are the important concluding points:

- The sensitivity of the algorithm to deviations in structural behavior is evident, emphasizing the importance of pre-emptively identifying potential failure modes for safeguarding structural integrity.
- The convergence toward optimized values, driven by a targeted reliability index ($\beta_{\text{target}} = 3.00$), showcases the efficacy of reliability-based optimization in tailoring beam designs to meet stringent reliability constraints.
- The derived values of web thickness (t_w) and flange thickness (t_f) ensure stability under the specified conditions and suggest an efficient utilization of materials, a crucial consideration in sustainable steel structure design.

- The stress distribution within the optimized configurations demonstrates notable improvements, particularly in reducing zones exhibiting yielded stress, ensuring structural integrity and averting plastic accumulation.

This work provides a significant foundation for further exploration in the nonlinear probabilistic analysis of sinusoidal-web steel beams. Future research endeavors should consider extending this approach to address additional nonlinear issues. Incorporating nonlinear material behavior into reliability-based optimization design could enhance the accuracy of our results, albeit at the cost of increased complexity. Nonlinear material behavior introduces additional challenges in terms of computational resources and algorithmic complexity. It could potentially influence reliability indices by altering the structural response under varying loading conditions. Future research endeavors could explore the feasibility and implications of incorporating nonlinear material behavior into a reliability-based optimization design for steel beams.

Author Contributions: Conceptualization, I.C.; validation, I.C., M.H. and M.M.R.; formal analysis, I.C. and J.S.; resources, J.S.; writing—original draft preparation, I.C. and M.H.; writing—review and editing, J.S. and M.M.R.; software, M.H. and M.M.R.; visualization, J.S.; investigation, J.S. and M.H.; supervision, I.C. and M.M.R.; methodology, I.C. and M.H.; All authors have read and agreed to the published version of the manuscript.

Funding: The research leading to these results was funded by 2020-1.1.2-Piaci-KFI-2 021-00231 in Hungary.

Data Availability Statement: The raw data supporting the conclusions of this article will be made available by the authors on request.

Acknowledgments: The authors would like to express their gratitude to the TRANSPORT-BETON KFT in Hungary for providing the sinusoidal-web beams used in the experimental tests.

Conflicts of Interest: The authors declare no conflicts of interest.

References

1. Zhao, J.; Yang, J. Overall Stability Behavior and Design Method of Q460 High Strength Steel Welded I-Section Overhanging Beams. *Thin-Walled Struct.* **2023**, *186*, 110665. [[CrossRef](#)]
2. Lindner, J. Design of Steel Beams and Beam Columns. *Eng. Struct.* **1997**, *19*, 378–384. [[CrossRef](#)]
3. Poologanathan, K.; Perampalam, G.; Gunalan, S.; Corradi, M. Structural Performance of Cold-Formed Steel (CFS) Structures. *Buildings* **2023**, *13*, 1689. [[CrossRef](#)]
4. Rad, M.M. A Review of Elasto-Plastic Shakedown Analysis with Limited Plastic Deformations and Displacements. *Period. Polytech. Civ. Eng.* **2018**, *62*, 812–817. [[CrossRef](#)]
5. Śledziewski, K.; Górecki, M. Finite Element Analysis of the Stability of a Sinusoidal Web in Steel and Composite Steel-Concrete Girders. *Materials* **2020**, *13*, 1041. [[CrossRef](#)] [[PubMed](#)]
6. Papangelis, J.; Trahair, N.; Hancock, G. Direct Strength Method for Shear Capacity of Beams with Corrugated Webs. *J. Constr. Steel Res.* **2017**, *137*, 152–160. [[CrossRef](#)]
7. Driver, R.G.; Abbas, H.H.; Sause, R. Shear Behavior of Corrugated Web Bridge Girders. *J. Struct. Eng.* **2006**, *132*, 195–203. [[CrossRef](#)]
8. Hassanein, M.F.; Elkawas, A.A.; El Hadidy, A.M.; Elchalakani, M. Shear Analysis and Design of High-Strength Steel Corrugated Web Girders for Bridge Design. *Eng. Struct.* **2017**, *146*, 18–33. [[CrossRef](#)]
9. Ibrahim, S.A.; El-Dakhakhni, W.W.; Elgaaly, M. Fatigue of Corrugated-Web Plate Girders: Experimental Study. *J. Struct. Eng.* **2006**, *132*, 1371–1380. [[CrossRef](#)]
10. Pasternak, H.; Kubieniec, G. Plate Girders with Corrugated Webs. *J. Civ. Eng. Manag.* **2010**, *16*, 166–171. [[CrossRef](#)]
11. de Carvalho, A.S.; Martins, C.H.; Rossi, A.; de Oliveira, V.M.; Morkhade, S.G. Moment Gradient Factor for Steel I-Beams with Sinusoidal Web Openings. *J. Constr. Steel Res.* **2023**, *202*, 107775. [[CrossRef](#)]
12. Reinders, P.; Balomenos, G.P. Lateral Torsional Buckling of Corrugated Web Plate Girders with Sinusoidal Web Profiles. *Pract. Period. Struct. Des. Constr.* **2022**, *27*, 04022051. [[CrossRef](#)]
13. de Carvalho, A.S.; Hosseinpour, M.; Rossi, A.; Martins, C.H.; Sharifi, Y. New Formulas for Predicting the Lateral–Torsional Buckling Strength of Steel I-Beams with Sinusoidal Web Openings. *Thin-Walled Struct.* **2022**, *181*, 110067. [[CrossRef](#)]
14. Wang, S.; He, J.; Liu, Y. Shear Behavior of Steel I-Girder with Stiffened Corrugated Web, Part I: Experimental Study. *Thin-Walled Struct.* **2019**, *140*, 248–262. [[CrossRef](#)]
15. Lee, S.H.; Park, G.W.; Yoo, J.H. Analytical Study of Shear Buckling Behavior of Trapezoidal and Sinusoidal Corrugated Web Girders. *Int. J. Steel Struct.* **2020**, *20*, 525–537. [[CrossRef](#)]

16. Zhang, Z.; Pei, S.; Qu, B. Cantilever Welded Wide-Flange Beams with Sinusoidal Corrugations in Webs: Full-Scale Tests and Design Implications. *Eng. Struct.* **2017**, *144*, 163–173. [[CrossRef](#)]
17. Pathirana, S.; Qiao, P. Elastic Local Buckling of Periodic Sinusoidal Corrugated Composite Panels Subjected to In-Plane Shear. *Thin-Walled Struct.* **2020**, *157*, 107134. [[CrossRef](#)]
18. Nikoomanesh, M.R.; Goudarzi, M.A. Experimental and Numerical Evaluation of Shear Load Capacity for Sinusoidal Corrugated Web Girders. *Thin-Walled Struct.* **2020**, *153*, 106798. [[CrossRef](#)]
19. Kim, K.; Park, S.J. Analysis of Shear Buckling for Sinusoidal Corrugated Web Beam. *Mech. Based Des. Struct. Mach.* **2023**, *51*, 6863–6880. [[CrossRef](#)]
20. Sebastiao, L.; Papangelis, J. Elastic Local Shear Buckling of Beams with Sinusoidal Corrugated Webs. *Structures* **2023**, *54*, 684–692. [[CrossRef](#)]
21. Wang, P.Y.; Garlock, M.E.M.; Zoli, T.P.; Quiel, S.E. Low-Frequency Sinusoids for Enhanced Shear Buckling Performance of Thin Plates. *J. Constr. Steel Res.* **2021**, *177*, 106475. [[CrossRef](#)]
22. Górecki, M.; Śledziewski, K. Experimental Investigation of Impact Concrete Slab on the Bending Behavior of Composite Bridge Girders with Sinusoidal Steel Web. *Materials* **2020**, *13*, 273. [[CrossRef](#)] [[PubMed](#)]
23. Szép, J.; Habashneh, M.; Lógó, J.; Movahedi Rad, M. Reliability Assessment of Reinforced Concrete Beams under Elevated Temperatures: A Probabilistic Approach Using Finite Element and Physical Models. *Sustainability* **2023**, *15*, 6077. [[CrossRef](#)]
24. Dániel, H.; Habashneh, M.; Rad, M.M. Reliability-Based Numerical Analysis of Glulam Beams Reinforced by CFRP Plate. *Sci. Rep.* **2022**, *12*, 13587. [[CrossRef](#)] [[PubMed](#)]
25. Benjamin, J.R.; Cornell, C.A. *Probability, Statistics, and Decision for Civil Engineers*; Courier Corporation: North Chelmsford, MA, USA, 2014.
26. Movahedi, R.A.D.M.; Lógó, J. Plastic Behaviour and Stability Constraints in the Reliability Based Shakedown Analysis and Optimal Design of Skeletal Structures. *Civ. Comp Proc.* **2010**, *203*, 1–14.
27. Pimenta, R.J.; Queiroz, G.; Diniz, S.M.C. Reliability-Based Design Recommendations for Sinusoidal-Web Beams Subjected to Lateral-Torsional Buckling. *Eng. Struct.* **2015**, *84*, 195–206. [[CrossRef](#)]
28. Leblouba, M.; Tabsh, S.W. Reliability-Based Shear Design of Corrugated Web Steel Beams for AISC 360 Specification and CSA-S16 Standard. *Eng. Struct.* **2020**, *215*, 110617. [[CrossRef](#)]
29. Bärnkopf, E.; Jáger, B.; Kövesdi, B. Lateral–Torsional Buckling Resistance of Corrugated Web Girders Based on Deterministic and Stochastic Nonlinear Analysis. *Thin-Walled Struct.* **2022**, *180*, 109880. [[CrossRef](#)]
30. Pimenta, R.J.; Diniz, S.M.C.; Queiroz, G.; Fakury, R.H.; Galvão, A.; Rodrigues, F.C. Reliability-Based Design Recommendations for Composite Corrugated-Web Beams. *Probabilistic Eng. Mech.* **2012**, *28*, 185–193. [[CrossRef](#)]
31. Habashneh, M.; Rad, M.M. Reliability Based Topology Optimization of Thermoelastic Structures Using Bi-Directional Evolutionary Structural Optimization Method. *Int. J. Mech. Mater. Des.* **2023**, *19*, 605–620. [[CrossRef](#)]
32. Movahedi Rad, M.; Habashneh, M.; Lógó, J. Reliability Based Bi-Directional Evolutionary Topology Optimization of Geometric and Material Nonlinear Analysis with Imperfections. *Comput. Struct.* **2023**, *287*, 107120. [[CrossRef](#)]
33. Zhang, W.; Li, Y.; Zhou, Q.; Qi, X.; Widera, G.E.O. Optimization of the Structure of an H-Beam with Either a Flat or a Corrugated Web: Part 3. Development and Research on H-Beams with Wholly Corrugated Webs. *J. Mater. Process. Technol.* **2000**, *101*, 119–123. [[CrossRef](#)]
34. Sokołowski, D.; Kamiński, M. Stochastic Reliability-Based Design Optimization Framework for the Steel Plate Girder with Corrugated Web Subjected to Corrosion. *Materials* **2022**, *15*, 7170. [[CrossRef](#)] [[PubMed](#)]
35. Shon, S.; Yoo, M.; Kang, J.; Lee, S. Minimum Weight Design of Sinusoidal Corrugated Web Beam Using Differential Evolution Algorithm. *Int. J. Steel Struct.* **2015**, *15*, 213–225. [[CrossRef](#)]
36. Shon, S.-D.M.-N.S.-J.J.-W. Development of Optimum Design Program of Sinusoidal Corrugated Web Beam Using Differential Evolution Algorithm. *J. Archit. Inst. Korea Struct. Constr.* **2013**, *29*, 21–28. [[CrossRef](#)]
37. Lee, D.; Shon, S.; Lee, S. Discrete Optimum Structural Design of the Sinusoidal Corrugated Web Beam Using DE. In Proceedings of the IASS 2016 Tokyo Symposium: Spatial Structures in the 21st Century, Tokyo, Japan, 26–30 September 2016.
38. Erdal, F.; Tunca, O.; Doğan, E. Optimum Design of Composite Corrugated Web Beams Using Hunting Search Algorithm. *Int. J. Eng. Appl. Sci.* **2017**, *9*, 156–168. [[CrossRef](#)]
39. Smith, M. *ABAQUS/Standard User's Manual, Version 6.9*; Dassault Systèmes Simulia Corp.: Johnston, RI, USA, 2009.
40. Stanton, A.; Wiegand, D.; Stanton, G. *Probability Reliability and Statistical Methods in Engineering Design*; John Wiley & Sons, Inc.: Hoboken, NJ, USA, 2000.
41. *EN1990*; Others Eurocode—Basis of Structural Design. BSI: London, UK, 2002.

Disclaimer/Publisher's Note: The statements, opinions and data contained in all publications are solely those of the individual author(s) and contributor(s) and not of MDPI and/or the editor(s). MDPI and/or the editor(s) disclaim responsibility for any injury to people or property resulting from any ideas, methods, instructions or products referred to in the content.